$B \to X_s l^+ l^-$ decay in a top quark two-Higgs-doublet model

Zhenjun Xiao*

Department of Physics and Institute of Theoretical Physics, Nanjing Normal University, Nanjing, Jiangsu 210097, People's Republic of China

Linxia Lü†

Department of Physics and Institute of Theoretical Physics, Nanjing Normal University, Nanjing, Jiangsu 210097, People's Republic of China

and Department of Physics, Nanyang Teacher's College, Nanyang, Henan 473061, People's Republic of China

(Received 9 May 2006; published 21 August 2006)

We calculate the new physics contributions to the rare semileptonic decay $B \to X_s l^+ l^-$ $(l = e, \mu)$ induced by the charged-Higgs loop diagrams appeared in the top quark two-Higgs doublet model (T2HDM). Within the considered parameter space, we found that (a) the effective Wilson coefficients $\tilde{C}_i^{\rm eff}(m_b)$ $(i = 7\gamma, 9V$ and $10A)$ in the T2HDM are always standard model-like; (b) the new physics contributions to $\tilde{C}_{7\gamma}^{\rm eff}$ and $\tilde{C}_{9V}^{\rm eff}$ can be significant in magnitude, but they tend to cancel each other; and (c) the T2HDM predictions for $\mathrm{Br}(B \to X_s l^+ l^-)$ agree well with the measured value within 1 standard deviation.

DOI: 10.1103/PhysRevD.74.034016 PACS numbers: 13.20.He, 12.15.Ji, 12.15.Lk, 12.60.Fr

I. INTRODUCTION

Flavor changing neutral current (FCNC) $b \to s$ processes are forbidden at the tree level in the standard model (SM). They proceed at a low rate via penguin or box diagrams. If additional diagrams with non-SM particles contribute to such a decay, their amplitudes will interfere with the SM amplitudes and thereby modify the rate as well as other properties. This feature makes FCNC processes an ideal place to search for new physics.

In the past decade, the data of $B \to X_s \gamma$ decay has served as one of the most important constraints for various new physics models beyond the SM. At present, the world average, $\mathrm{Br}(B \to X_s \gamma) = (3.55 \pm 0.26) \times 10^{-4}$ [1], agrees very well with the standard model prediction at next-next-to-leading order (NNLO) [2]. The magnitude of the Wilson coefficient $C_{7\gamma}(\mu_b)$ is therefore strongly constrained by the precision data of $B \to X_s \gamma$, but its sign is still to be determined through the measurement of $B \to X_s l^+ l^-$ decay [3]. In Ref. [3], the authors studied $B \to X_s l^+ l^-$ decay and found that the recent experimental data of $\mathrm{Br}(B \to X_s l^+ l^-)$ prefer a SM-like $C_{7\gamma}(\mu_b)$.

In fact, the semileptonic decays $B \to X_s l^+ l^-$ $(l = e, \mu)$ have been extensively investigated, for example, in the SM [4,5], the two-Higgs doublet models (2HDM) [6] or the supersymmetric models [7,8]. Our goal in the present work is to calculate the new physics contributions to the branching ratio of $B \to X_s \gamma$ and $B \to X_s l^+ l^-$ decays induced by the charged-Higgs loop diagrams in the top-quark two-Higgs-doublet model (T2HDM) [9–11], and compare the theoretical predictions in the T2HDM with currently available data.

The outline of the paper is as follows. In Sec. II, we give a brief review for the top-quark two-Higgs-doublet model and we calculate the new penguin diagrams induced by new particles and extract out the new physics parts of the Wilson coefficients or some basic functions in the T2HDM. In Sec. III, we present the numerical results of the branching ratios of $B \to X_s l^+ l^-$ decay in the SM and the T2HDM, and make phenomenological analysis. The conclusions are included in the final section.

II. THEORETICAL FRAMEWORK

A. Outline of the top quark two-Higgs-doublet model

The specific model considered here is the top quark two-Higgs-doublet model (T2HDM) proposed in Ref. [9] and studied in Refs. [10,11], which is also a special case of the 2HDM of type III [12]. In this model, the large mass of the top quark arises naturally in the extension of the SM since the top quark is the only fermion receiving its mass from the vacuum expectation value (VEV) of the second Higgs doublet. All the other fermions receive their masses from the VEV of the first Higgs doublet.

Let us now briefly recapitulate some important features of the model of Ref. [9]. Consider the Yukawa Lagrangian of the form:

$$\mathcal{L}_Y = -\bar{L}_L \phi_1 E l_R - \bar{Q}_L \phi_1 F d_R - \bar{Q}_L \tilde{\phi}_1 G \mathbf{1}^{(1)} u_R - \bar{Q}_L \tilde{\phi}_2 G \mathbf{1}^{(2)} u_R + \mathrm{H.c.}, \quad (1)$$

where Q_L and L_L are 3-vector of the left-handed quark and lepton doublets, respectively; ϕ_i $(i = 1, 2)$ are the two Higgs doublets with $\tilde{\phi}_i = i\tau_2 \phi_i^*$; and E, F,G are the 3×3 matrices in the generation space and give masses, respectively, to the charged leptons, the down and up-type quarks; $\mathbf{1}^{(1)} \equiv \mathrm{diag}(1, 1, 0)$; $\mathbf{1}^{(2)} \equiv \mathrm{diag}(0, 0, 1)$ are the two

*Electronic address: xiaozhenjun@njnu.edu.cn
†Electronic address: lulinxia@email.njnu.edu.cn

orthogonal projection operators onto the first two and the third families, respectively. The top quark is assigned a special status by coupling it to one Higgs doublet that gets a large VEV, whereas all the other quarks are coupled only to the other Higgs doublet whose VEV is much smaller. Consequently, if one sets the VEVs of ϕ_1 and ϕ_2 to be $v_1/\sqrt{2}$ and $v_2 e^{i\theta}/\sqrt{2}$ [9], the ratio of two Higgs VEVs, $\tan\beta = v_2/v_1$, is required to be relatively large.

The Yukawa couplings involving the charged-Higgs bosons are of the form [9]

$$\begin{aligned}\mathcal{L}_Y^C = \frac{g}{\sqrt{2}M_W}\{&-\bar{u}_L V M_D d_R[G^+ - \tan\beta H^+] \\ &+ \bar{u}_R M_U V d_L[G^+ - \tan\beta H^+] \\ &+ \bar{u}_R \Sigma^\dagger V d_L[\tan\beta + \cot\beta]H^+ + \text{H.c.}\},\end{aligned} \tag{2}$$

where $G^\pm$ and $H^\pm$ denote the would-be Goldstone bosons and the physical charged Higgs bosons, respectively. Here M_U and M_D are the diagonal up- and down-type mass matrices, V is the usual CKM matrix and $\Sigma \equiv M_U U_R^\dagger \mathbf{1}^{(2)} U_R$. $U_R^\dagger$ is the unitary matrix which diagonalizes the right-handed up-type quarks and has the following form:

$$\begin{aligned}U_R = &\begin{pmatrix}\cos\phi & -\sin\phi & 0\\ \sin\phi & \cos\phi & 0\\ 0 & 0 & 1\end{pmatrix} \\ &\times\begin{pmatrix}1 & 0 & 0\\ 0 & \sqrt{1-|\epsilon_{ct}\xi|^2} & -\epsilon_{ct}\xi^* \\ 0 & \epsilon_{ct}\xi & \sqrt{1-|\epsilon_{ct}\xi|^2}\end{pmatrix},\end{aligned} \tag{3}$$

where $\epsilon_{ct} \equiv m_c/m_t$, $\xi = |\xi|e^{i\delta}$ is a complex number of order unity, and the phase δ in ξ is a new CP violating phase. Inserting Eq. (3) into the definition of Σ yields

$$\Sigma = \begin{pmatrix}0 & 0 & 0\\ 0 & m_c\epsilon_{ct}^2|\xi|^2 & m_c\epsilon_{ct}\xi^*\sqrt{1-|\epsilon_{ct}\xi|^2} \\ 0 & m_c\xi\sqrt{1-|\epsilon_{ct}\xi|^2} & m_t(1-|\epsilon_{ct}\xi|^2)\end{pmatrix}. \tag{4}$$

In the following sections, we will calculate the charged Higgs contributions to the rare decay $B \to X_s l^+ l^-$ in the top quark two-Higgs-doublet model.

B. Effective Hamiltonian for $B \to X_s l^+ l^-$ in the SM

In the framework of the SM, the effective Hamiltonian inducing the transition $b \to s l^+ l^-$ at the scale μ can be written as follows:

$$\mathcal{H} = -\frac{4G_F}{\sqrt{2}} V_{ts}^* V_{tb} \sum_{i=1}^{10} C_i(\mu) Q_i(\mu), \tag{5}$$

where G_F is the coupling constant, and $V_{ts}^* V_{tb}$ is the Cabibbo-Kobayashi-Maskawa (CKM) factor [13]. The operators can be chosen as Ref. [4]

$$\begin{aligned}Q_1 &= (\bar{s}_L\gamma_\mu T^a c_L)(\bar{c}_L\gamma^\mu T^a b_L),\\ Q_2 &= (\bar{s}_L\gamma_\mu c_L)(\bar{c}_L\gamma^\mu b_L),\\ Q_3 &= (\bar{s}_L\gamma_\mu b_L)\sum_q(\bar{q}\gamma^\mu q),\\ Q_4 &= (\bar{s}_L\gamma_\mu T^a b_L)\sum_q(\bar{q}\gamma^\mu T^a q),\\ Q_5 &= (\bar{s}_L\gamma_{\mu_1}\gamma_{\mu_2}\gamma_{\mu_3} b_L)\sum_q(\bar{q}\gamma^{\mu_1}\gamma^{\mu_2}\gamma^{\mu_3} q),\\ Q_6 &= (\bar{s}_L\gamma_{\mu_1}\gamma_{\mu_2}\gamma_{\mu_3} T^a b_L)\sum_q(\bar{q}\gamma^{\mu_1}\gamma^{\mu_2}\gamma^{\mu_3} T^a q),\\ Q_{7\gamma} &= \frac{e}{g_s^2} m_b(\bar{s}_L\sigma^{\mu\nu} b_R)F_{\mu\nu},\\ Q_{8g} &= \frac{1}{g_s} m_b(\bar{s}_L\sigma^{\mu\nu} T^a b_R)G^a_{\mu\nu},\\ Q_{9V} &= \frac{e^2}{g_s^2}(\bar{s}_L\gamma_\mu b_L)\sum_\ell(\bar{\ell}\gamma^\mu \ell),\\ Q_{10A} &= \frac{e^2}{g_s^2}(\bar{s}_L\gamma_\mu b_L)\sum_\ell(\bar{\ell}\gamma^\mu\gamma_5 \ell),\end{aligned} \tag{6}$$

where $Q_{1,2}$ are the current-current operators, Q_{3-6} the QCD penguin operators, $Q_{7,8}$ "magnetic penguin" operators, and $Q_{9,10}$ semileptonic electroweak penguin operators. $T^a (a = 1, \ldots, 8)$ stands for $SU(3)_c$ generators, L, $R \equiv (1 \mp \gamma_5)/2$ by definition. The sum over q runs over the quark fields that are active at the scale $\mu = \mathcal{O}(m_b)$, i.e., $q \in \{u, d, s, c, b\}$. We work in the approximation where the combination $(V_{us}^* V_{ub})$ of the CKM matrix elements is neglected. We do not separate top-quark and charm-quark contributions and will give the results in the summed form.

To calculate the semileptonic B meson decays at next-to-leading order in α_s, we should determinate the Wilson coefficient $C_i(M_W)$ through matching of the full theory onto the five-quark low energy effective theory where the $W^\pm$ gauge boson, top quark and the new particles of T2HDM heavier than M_W are integrated out, and run the Wilson coefficients down to the low energy scale $\mu \sim \mathcal{O}(m_b)$ by using the QCD renormalization group equations. The corresponding Wilson coefficients in SM can be found, for example, in Refs. [14,15].

C. New physics contributions

In the framework of the SM, the semileptonic $B \to X_s l^+ l^-$ $(l = e^-, \mu^-)$ decays proceed through loop diagrams and are of forth order in the weak coupling. The dominant contributions to this decay come from the W box and Z penguin diagrams. The corresponding one-loop diagrams in the SM were evaluated long time ago and can be found in Refs. [4,16]. The calculations at the next-next-to-leading order (NNLO) are also available now.

In the T2HDM considered here, besides the SM diagrams with a W-gauge boson and an up quark in the loop,

the $B \to X_s l^+ l^-$ decays can also proceed via the new diagrams involving the charged-Higgs boson exchanges, as illustrated by Fig. 1. In order to determine the new physics contributions to the relevant Wilson coefficients $C_{7\gamma}$, C_{8g}, C_{9V}, and C_{10A} at the M_W scale, we need to calculate the corresponding Feynman diagrams.

The new physics parts of the Wilson coefficients $C_{7\gamma}$ and C_{8g} have been calculated in Refs. [10,11] and confirmed by our independent calculation. In the naive dimensional regularization (NDR) scheme, they are of the form

$$C_{7\gamma}^{\rm NP}(M_W) = \sum_{i=c,t} \kappa^{\rm is}\Big[-\tan^2\beta + \frac{1}{m_i V_{\rm is}^*}(\Sigma^T V^*)_{\rm is}(\tan^2\beta+1)\Big] \times \Big\{B(y_i) + \frac{1}{6}A(y_i)\Big[-1 + \frac{1}{m_i V_{\rm ib}}(\Sigma^\dagger V)_{\rm ib} \times (\cot^2\beta+1)\Big]\Big\}, \quad (7)$$

$$C_{8g}^{\rm NP}(M_W) = \sum_{i=c,t} \kappa^{\rm is}\Big[-\tan^2\beta + \frac{1}{m_i V_{\rm is}^*}(\Sigma^T V^*)_{\rm is}(\tan^2\beta+1)\Big] \times \Big\{E(y_i) + \frac{1}{6}F(y_i)\Big[-1 + \frac{1}{m_i V_{\rm ib}}(\Sigma^\dagger V)_{\rm ib} \times (\cot^2\beta+1)\Big]\Big\}, \quad (8)$$

with the Inami-Lim functions

$$A(y) = \frac{7y-5y^2-8y^3}{12(1-y)^3} + \frac{2y^2-3y^3}{2(1-y)^4}\ln[y],$$
$$B(y) = \frac{-3y+5y^2}{12(1-y)^2} - \frac{2y-3y^2}{6(1-y)^3}\ln[y],$$
$$E(y) = \frac{-3y+y^2}{4(1-y)^2} - \frac{y}{2(1-y)^3}\ln[y], \quad (9)$$
$$F(y) = \frac{2y+5y^2-y^3}{4(1-y)^3} + \frac{3y^2}{2(1-y)^4}\ln[y],$$

where $\kappa^{\rm is} = -V_{\rm ib}V_{\rm is}^*/(V_{tb}V_{ts}^*)$, $y_i = (m_i/m_H)^2$.

As for the Wilson coefficients C_{9V}, and C_{10A} at the M_W scale, we found the new physics parts after calculating analytically the Feynman diagrams as shown in Fig. 1,

$$C_{9V}^{\rm NP}(M_W) = \frac{1}{\sin^2\theta_W}[C_0^{\rm NP} - B_0^{\rm NP}] - [D_0^{\rm NP} + 4C_0^{\rm NP}], \quad (10)$$

$$C_{10A}^{\rm NP}(M_W) = -\frac{1}{\sin^2\theta_W}[C_0^{\rm NP} - B_0^{\rm NP}], \quad (11)$$

where

$$B_0^{\rm NP} = -\frac{m_l m_b \tan^2\beta}{8M_W^2} B_+(x_{H^+}, x_t), \quad (12)$$

$$C_0^{\rm NP} = \sum_{i=c,t} \kappa^{\rm is}\frac{m_i^2}{8M_W^2}\Big\{\Big[C'_{01}(y_i) - \frac{4m_b^2}{3m_i^2}\sin^2\theta_W C'_{11}(y_i)\Big]\Big[-\tan^2\beta + \frac{1}{m_i V_{\rm is}^*}(\Sigma^T V^*)_{\rm is}(\tan^2\beta+1)\Big]\Big[-1 + \frac{1}{m_i V_{\rm ib}}(\Sigma^\dagger V)_{\rm ib} \times (\cot^2\beta+1)\Big] + \frac{m_b^2}{m_i^2}\Big[\Big(1-\frac{4}{3}\sin^2\theta_W\Big)C'_{01}(y_i) - C'_{11}(y_i)\Big]\Big[-\tan^2\beta + \frac{1}{m_i V_{\rm is}^*}(\Sigma^T V^*)_{\rm is}(\tan^2\beta+1)\Big]\Big\}, \quad (13)$$

$$D_0^{\rm NP} = \sum_{i=c,t} \kappa^{\rm is}\frac{2H(y_i)}{3}\Big[-\tan^2\beta + \frac{1}{m_i V_{\rm is}^*}(\Sigma^T V^*)_{\rm is}(\tan^2\beta+1)\Big]\Big[-1 + \frac{1}{m_i V_{\rm ib}}(\Sigma^\dagger V)_{\rm ib}(\cot^2\beta+1)\Big], \quad (14)$$

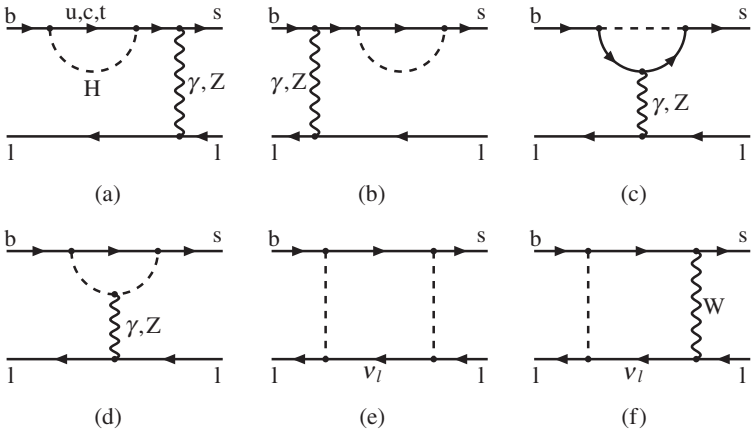

FIG. 1. The typical Feynman diagrams for the decay $B \to X_s l^+ l^-$ in the T2HDM. The internal solid and dashed lines denote the propagators of upper quarks (u,c,t) and charged-Higgs boson, respectively.

with

$$B_+(x,z) = \frac{z}{x-z}\left[\frac{\ln[z]}{z-1} - \frac{\ln[x]}{x-1}\right],$$
$$H(y) = \frac{38y - 79y^2 + 47y^3}{72(1-y)^3} + \frac{4y - 6y^2 + 3y^4}{12(1-y)^4}\ln[y],$$
$$C'_{01}(y) = \frac{y}{1-y} + \frac{y}{(1-y)^2}\ln[y],$$
$$C'_{11}(y) = \frac{3y - y^2}{4(1-y)^2} + \frac{y}{2(1-y)^3}\ln[y], \quad (15)$$

where $y_i = m_i^2/m_H^2$, $x_{H^+} = m_H^2/M_W^2$, and $x_t = m_t^2/M_W^2$. V is the CKM matrix, and the matrix Σ has been given in Eq. (4). The contributions from Fig. 1(e) and the Fig. 1(f) when the internal W and charged-Higgs lines exchange their position are strongly suppressed by a factor of $(m_l/m_H)^2$ $(m_l = m_e, m_\mu)$ or m_s/m_b, and therefore have been neglected.

D. The differential decay rate

Within the standard model, the differential decay rate for the decay $B \to X_s l^+ l^-$ in the NNLO approximation can be written as [5,17]

$$R(\hat{s}) \equiv \frac{\frac{d}{d\hat{s}}\Gamma(b \to s l^+ l^-)}{\Gamma(b \to c e \overline{\nu})} = \frac{\alpha_{\rm em}^2}{4\pi^2}\left|\frac{V_{ts}^* V_{tb}}{V_{cb}}\right|^2 \frac{(1-\hat{s})^2}{f(z)\kappa(z)}\Big[(1+2\hat{s})(|\tilde{C}_{9V}^{\rm eff}(\hat{s})|^2 + |\tilde{C}_{10A}^{\rm eff}(\hat{s})|^2) + 4\left(1+\frac{2}{\hat{s}}\right)|\tilde{C}_{7\gamma}^{\rm eff}|^2 + 12\,{\rm Re}[\tilde{C}_{7\gamma}^{\rm eff}(\tilde{C}_{9V}^{\rm eff}(\hat{s}))^*]\Big], \quad (16)$$

where

$$\tilde{C}_k^{\rm eff} = -\hat{C}_k^{\rm eff} + \frac{V_{us}^* V_{ub}}{V_{ts}^* V_{tb}}\delta_{k9}\Delta\hat{C}_9^{\rm eff} \quad (17)$$

that are related to the evolved coefficients $C_k(\mu_b)$ as follows:

$$\hat{C}_{7\gamma}^{\rm eff} = \frac{4\pi}{\alpha_s(\mu_b)}C_7(\mu_b) - \frac{1}{3}C_3(\mu_b) - \frac{4}{9}C_4(\mu_b) - \frac{20}{3}C_5(\mu_b) - \frac{80}{9}C_6(\mu_b), \quad (18)$$

$$\hat{C}_{9V}^{\rm eff}(\hat{s}) = 4C_9(\mu_b)\left(\frac{\pi}{\alpha_s(\mu_b)} + \omega(\hat{s})\right) + \sum_{i=1}^{6} C_i(\mu_b)\gamma_{i9}^{(0)}\ln\frac{m_b}{\mu_b} + h\left(\frac{m_c^2}{m_b^2},\hat{s}\right)\left[\frac{4}{3}C_1(\mu_b) + C_2(\mu_b) + 6C_3^Q(\mu_b) + 60C_5^Q(\mu_b)\right] + h(1,\hat{s})\left(-\frac{7}{2}C_3(\mu_b) - \frac{2}{3}C_4(\mu_b) - 38C_5(\mu_b) - \frac{32}{3}C_6(\mu_b)\right) + h(0,\hat{s})\left(-\frac{1}{2}C_3(\mu_b) - \frac{2}{3}C_4(\mu_b) - 8C_5(\mu_b) - \frac{32}{3}C_6(\mu_b)\right) + \frac{4}{3}C_3(\mu_b) + \frac{64}{9}C_5(\mu_b) + \frac{64}{27}C_6(\mu_b), \quad (19)$$

$$\hat{C}_{10A}^{\rm eff}(\hat{s}) = 4C_{10}(\mu_b)\left(\frac{\pi}{\alpha_s(\mu_b)} + \omega(\hat{s})\right), \quad (20)$$

$$\Delta\hat{C}_{9V}^{\rm eff} = \left[h(0,\hat{s}) - h\left(\frac{m_c^2}{m_b^2},\hat{s}\right)\right]\left(\frac{4}{3}C_1(\mu_b) + C_2(\mu_b)\right), \quad (21)$$

with

$$h(z,\hat{s}) = -\frac{4}{9}\ln z + \frac{8}{27} + \frac{4}{9}x - \frac{2}{9}(2+x) \times\sqrt{|1-x|}\begin{cases}\ln\left|\frac{\sqrt{1-x}+1}{\sqrt{1-x}-1}\right| - i\pi, & \text{for } x \equiv 4z/\hat{s} < 1,\\ 2\arctan(1/\sqrt{x-1}), & \text{for } x \equiv 4z/\hat{s} > 1,\end{cases} \quad (22)$$

$$h(0,\hat{s}) = \frac{8}{27} - \frac{4}{9}(\ln\hat{s} - i\pi),$$
$$\omega(\hat{s}) = -\frac{4}{3}Li_2(\hat{s}) - \frac{2}{3}\ln(1-\hat{s})\ln\hat{s} - \frac{2}{9}\pi^2 - \frac{5+4\hat{s}}{3(1+2\hat{s})}\ln(1-\hat{s}), \quad (23)$$

$$- \frac{2\hat{s}(1+\hat{s})(1-2\hat{s})}{3(1-\hat{s})^2(1+2\hat{s})}\ln\hat{s} + \frac{5+9\hat{s}-6\hat{s}^2}{6(1-\hat{s})(1+2\hat{s})}, \quad (24)$$

and

$$f(z) = 1 - 8z^2 + 8z^6 - z^8 - 24z^4\ln z, \quad (25)$$

$$\kappa(z) \simeq 1 - \frac{2\alpha_s(\mu)}{3\pi}\left[\left(\pi^2 - \frac{31}{4}\right)(1-z)^2 + \frac{3}{2}\right]. \quad (26)$$

Here $\hat{s} = (p_{l^+} + p_{l^-})^2/m_b^2 = m_{ll}^2/m_b^2$, $z = m_c/m_b$, $f(z)$ and $\kappa(z)$ are the phase-factor and single gluon QCD correction to the $b \to c e \bar{\nu}$ decay, respectively.

In Refs. [17], the Wilson coefficients have been expanded perturbatively as follows

$$C_i = C_i^{(0)} + \frac{g_s^2}{(4\pi)^2} C_i^{(1)} + \frac{g_s^4}{(4\pi)^4} C_i^{(2)} + \mathcal{O}(g^6). \quad (27)$$

For the standard model parts of the Wilson coefficients $C_i^{(0)}$, $C_i^{(1)}$ and $C_i^{(2)}$, the explicit expressions as given in Refs. [5,17] will be used in our numerical calculation. For the new physics part, only $C_i^{(1)\mathrm{NP}}(M_W)$ are known at present, as given explicitly in Eqs. (7), (8), (10), and (11), and will be included in numerical calculations.

III. NUMERICAL RESULT

In this section, we first give the input parameters needed in numerical calculations, and then present the numerical results and make some theoretical analysis.

A. Input parameters

In numerical calculations we will use the following input parameters (all masses are in GeV) [18]:

$$\begin{aligned} &M_W = 80.425, \quad G_F = 1.16639 \times 10^{-5}\ \mathrm{GeV}^{-2}, \\ &\alpha_{\mathrm{em}} = 1/128, \quad m_c = 1.4, \quad m_b = 4.8 \pm 0.2, \\ &m_t = 173.8 \pm 5, \quad \Lambda_{\overline{\mathrm{MS}}}^{(5)} = 0.225, \quad A = 0.853, \\ &\lambda = 0.2200, \quad \rho = 0.20 \pm 0.09, \\ &\eta = 0.33 \pm 0.05, \quad \sin^2\theta_W = 0.23124, \\ &Br(B \to X_c e \bar{\nu}) = 0.1061, \end{aligned} \quad (28)$$

where the parameter A, λ, ρ and η are Wolfenstein parameters of the CKM mixing matrix. For the strong coupling constant $\alpha_s(\mu)$ we use the two-loop expression,

$$\alpha_s(\mu) = \frac{4\pi}{\beta_0 \ln(\mu^2/\Lambda_{\overline{\mathrm{MS}}}^2)}\left[1 - \frac{\beta_1}{\beta_0^2} \cdot \frac{\ln\ln(\mu^2/\Lambda_{\overline{\mathrm{MS}}}^2)}{\ln(\mu^2/\Lambda_{\overline{\mathrm{MS}}}^2)}\right], \quad (29)$$

with

$$\beta_0 = \frac{33 - 2f}{3}, \qquad \beta_1 = 72 - 10f - 8f/3, \quad (30)$$

where the f is the number of quark flavors, and the term $\overline{\mathrm{MS}}$ denotes the modified subtraction scheme.

B. $B \to X_s\gamma$ decay

There are four free parameters m_H, $\tan\beta$, $|\xi|$ and a new CP-violating phase δ in the T2HDM. We fix $|\xi| = 1$ throughout the paper and consider other three as variable parameters to be constrained by precise measurements, such as the date of $\mathrm{Br}(B \to X_s\gamma)$.

In Ref. [19], the branching ratio $\mathrm{Br}(B \to X_s\gamma)$ have been calculated in both the SM and the T2HDM. Using the formulas as given in Appendix A and taking the range of

$$2.77 \times 10^{-4} \le \mathrm{Br}(B \to X_s\gamma) \le 4.33 \times 10^{-4} \quad (31)$$

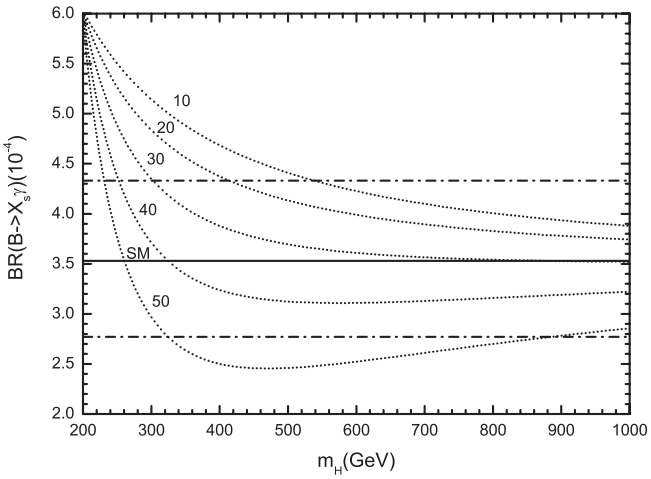

FIG. 2. The m_H dependence of $\mathrm{Br}(B \to X_s\gamma)$ in the T2HDM for $\delta = 0°$, and for $\tan\beta = 10$, 20, 30, 40 and 50, respectively. The band between two horizontal dash dot lines shows data as specified in Eq. (31). The solid horizontal line shows the central value of the SM prediction.

as the experimentally allowed region at 3σ level [1], one can read off the lower limit on the mass of charged-Higgs boson m_H directly from Fig. 2:

$$m_H \ge 300\ \mathrm{GeV}, \quad (32)$$

for fixed $\tan\beta = 30$ and $\delta = 0°$. It is easy to see from Fig. 2 that (a) a light charged-Higgs boson with a mass less than 200 GeV is excluded by the data of $B \to X_s\gamma$ decay at 3σ level; and (b) a charged-Higgs boson with a mass heavier than 300 GeV is still allowed by the same data.

As shown in the contour plot Fig. 3, the region between the short-dashed and solid curves is still allowed by the data of $B \to X_s\gamma$ as given in Eq. (31) for fixed value of $\delta = 0°$. On the other hand, by assuming $\tan\beta = 30$ and $m_H = 400$ GeV, one finds a strong constraint on the phase δ: $\delta < 44°$.

C. $B \to X_s l^+ l^-$ decay

The branching ratio of $B \to X_s l^+ l^-$ ($l = e, \mu$) has been recently measured by *BABAR* and Belle Collaborations [20,21]. In the low-q^2 region,[1] the average of *BABAR* and Belle's measurements is [3]

$$\mathrm{Br}\,(B \to X_s l^+ l^-) = (1.60 \pm 0.51) \times 10^{-6}. \quad (33)$$

Theoretically, the integrated branching ratio can be written as [17]

$$\mathrm{Br}_{ll} = \mathrm{Br}(\bar{B} \to X_c l \nu) \int_{\hat{s}_a}^{\hat{s}_b} R(\hat{s}), \quad (34)$$

where $\hat{s} = q^2/m_b^2$ with $\hat{s}_a = 1/m_b^2$ and $\hat{s}_b = 6/m_b^2$, and the differential decay rate $R(\hat{s})$ has been defined in Eq. (16).

[1]The low-q^2 region is the region with $1\ \mathrm{GeV}^2 \le m_{ll}^2 \equiv q^2 \le 6\ \mathrm{GeV}^2$.

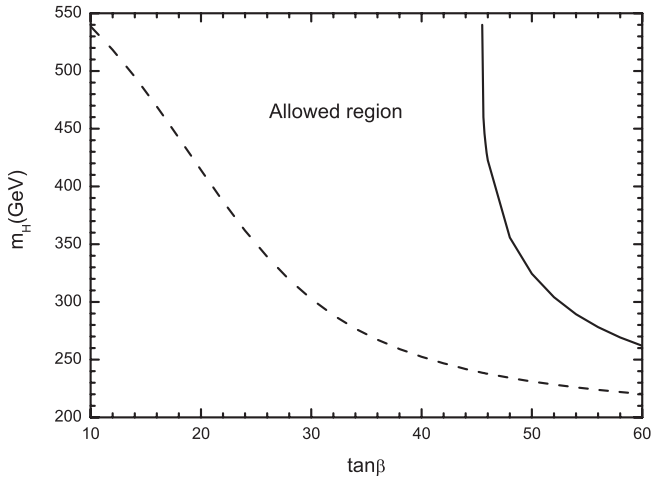

FIG. 3. Contour plot in $\tan\beta - m_H$ plane obtained by considering the data in Eq. (31) for fixed $\delta = 0$. The region between the short-dashed and solid curves is still allowed by the data as given in Eq. (31).

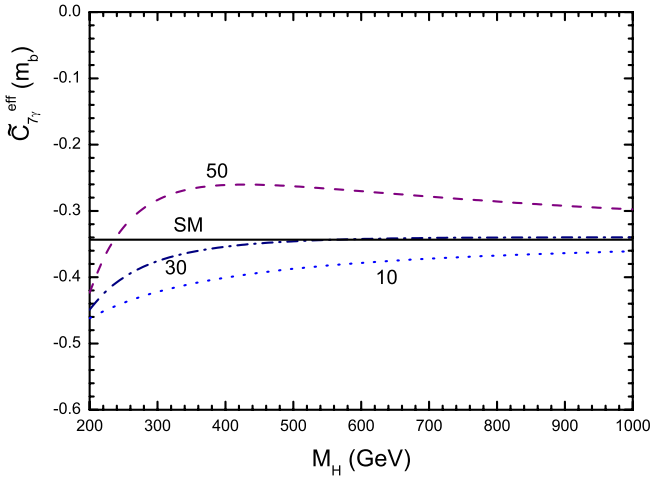

FIG. 4 (color online). The m_H dependence of the real part of the effective Wilson coefficient $\tilde{C}_{7\gamma}^{\rm eff}(m_b)$ in the SM (solid line) and T2HDM for $\delta = 0°$, and $\tan\beta = 10$ (dotted curve), 30 (dot-dashed curve) and 50 (dashed curve), respectively.

The SM prediction after integrating over the low-q^2 region reads

$$\begin{aligned}\mathrm{Br}(B \to X_s l^+ l^-) &= (1.58 \pm 0.08|_{m_t} \pm 0.07|_{\mu_b} \pm 0.04|_{\rm CKM} \\ &\quad \pm 0.06|_{m_b} + 0.18|_{\mu_w}) \times 10^{-6} \\ &= (1.58 \pm 0.13 + 0.18|_{\mu_w}) \times 10^{-6}, \quad (35)\end{aligned}$$

where the errors correspond to the uncertainty of input parameters of m_t, A, ρ, η and m_b as shown in Eq. (28), and for $m_b/2 \le \mu_b \le 2m_b$. The last error refers to the choice of $\mu_W = 120$ GeV, instead of $\mu_W = M_W$. Since we here focus on the new physics contributions to the branching ratios of $B \to X_s l^+ l^-$ decay, we will take $\mu_W = M_W$ in the following without further specification.

Now we consider the new physics contributions. When the new physics parts of the Wilson coefficients $C_i^{(1)(M_W)}$ for $i = 7\gamma, 8g, 9V$ and $10A$ are taken into account, the values of the effective Wilson coefficients appeared in Eq. (16) and the theoretical predictions of the branching ratio will be changed accordingly, as listed in Table I for $\tan\beta = 10$, 30, 50, $m_H = 300$ GeV and $\delta = 0°$, 30° and 60°.

In Figs. 4 and 5, in order to show more details of the m_H and $\tan\beta$ dependence, we draw the real part of the effective Wilson coefficients $\tilde{C}_{7\gamma}^{\rm eff}(m_b)$ and $\tilde{C}_{9V}^{\rm eff}(m_b)$ for fixed $\hat{s} = q^2/m_b^2 = 0.2$ and $\delta = 0°$. Within the considered parameter space of the T2HDM, it is easy to see from the numerical results in Table I and Figs. 4 and 5 that

(1) The effective Wilson coefficient $\tilde{C}_{7\gamma}^{\rm eff}(m_b)$ is always SM-like. This feature can be seen explicitly in Fig. 4, where the m_H-dependence of the real part of $\tilde{C}_{7\gamma}^{\rm eff}(m_b)$ is shown for $\delta = 0°$, $\tan\beta = 10$, 30, 50 and 200 GeV $\le m_H \le$ 1000 GeV. The imaginary part of $\tilde{C}_{7\gamma}^{\rm eff}(m_b)$ is generally small.

(2) The effective Wilson coefficient $\tilde{C}_{9V}^{\rm eff}(m_b)$ is also SM-like. The imaginary part of $\tilde{C}_{9V}^{\rm eff}(m_b)$ is also generally small.

TABLE I. The effective Wilson coefficients and the interference term ($12\,\mathrm{Re}[\tilde{C}_{7\gamma}^{\rm eff}(\tilde{C}_{9V}^{\rm eff})^*]$) for fixed $\hat{s} = q^2/m_b^2 = 0.2$, the branching ratio integrated over the low-q^2 region in units 10^{-6} in the SM and the T2HDM for $m_H = 300$, $\tan\beta = 10$, 30, 50 and (a) $\delta = 0°$, (b) 30° and (c) 60°. Only the central values are shown here.

	$\tilde{C}_{7\gamma}^{\rm eff}$	$\tilde{C}_{9V}^{\rm eff}$	$\tilde{C}_{10A}^{\rm eff}$	Int. Term	Br_{ll}
SM	-0.344	$4.302 + i0.064$	-3.547	-17.73	1.579
T2HDM	(a) $-0.422 + i0.001$	(a) $4.205 + i0.063$	(a) -3.552	-21.30	1.576
$\tan\beta = 10$	(b) $-0.424 + i0.006$	(b) $4.218 + i0.014$	(b) $-3.552 + i0.001$	-21.45	1.581
	(c) $-0.428 + i0.010$	(c) $4.255 - i0.021$	(c) $-3.553 + i0.001$	-21.84	1.595
	(a) $-0.376 + i0.001$	(a) $3.430 + i0.051$	(a) -3.546	-15.47	1.342
$\tan\beta = 30$	(b) $-0.389 + i0.050$	(b) $3.554 - i0.385$	(b) $-3.546 + i0.001$	-16.84	1.388
	(c) $-0.425 + i0.086$	(c) $3.879 - i0.700$	(c) $-3.547 + i0.002$	-20.50	1.581
	(a) $-0.283 + i0.002$	(a) $1.882 + i0.026$	(a) -3.544	-6.40	1.033
$\tan\beta = 50$	(b) $-0.321 + i0.140$	(b) $2.226 - i1.183$	(b) $-3.544 + i0.002$	-10.56	1.167
	(c) $-0.420 + i0.239$	(c) $3.126 - i2.056$	(c) $-3.546 + i0.003$	-21.65	1.526

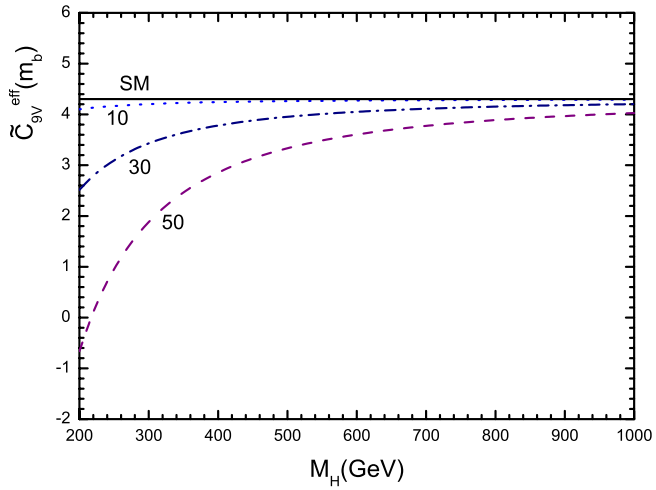

FIG. 5 (color online). The m_H dependence of the real part of the effective Wilson coefficient $\tilde{C}_{9V}^{\rm eff}(m_b)$ in the SM (solid line) and T2HDM for $\hat{s} = 0.2$, $\delta = 0°$, and $\tan\beta = 10$ (dotted curve), 30 (dot-dashed curve) and 50 (dashed curve), respectively.

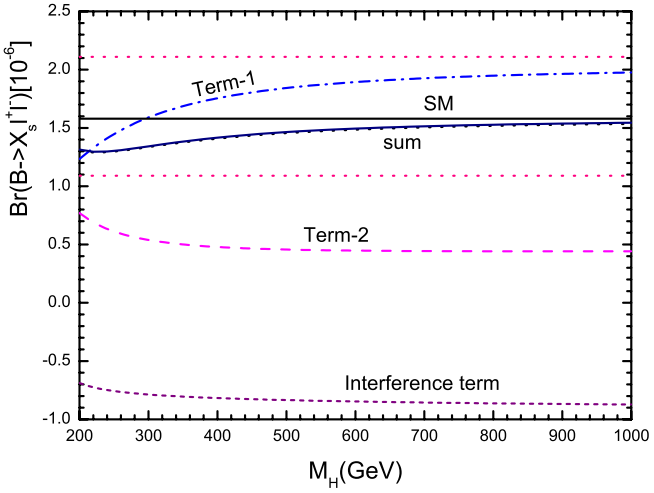

FIG. 6 (color online). The m_H dependence of the branching ratio of $B \to X_s l^+ l^-$ in the SM and T2HDM for $\delta = 0°$, and $\tan\beta = 30$. The contributions from the term-1, term-2, interference term and their summation are shown by the dot-dashed, dashed, short-dashed and solid curve, respectively. The horizontal band between two dotted lines shows the data: $\mathrm{Br}(B \to X_s l^+ l^-) = (1.60 \pm 0.51) \times 10^{-6}$, while the solid line refers to the central value of SM prediction: $\mathrm{Br}(B \to X_s l^+ l^-) = 1.58 \times 10^{-6}$.

(3) The new physics contribution to $\tilde{C}_{10A}^{\rm eff}$ is very small in size, less than 1% of its standard model counterpart, and therefore can be neglected safely.
(4) The new physics contributions to $\tilde{C}_{7\gamma}^{\rm eff}$ and $\tilde{C}_{9V}^{\rm eff}$ can be significant in magnitude, respectively, for large $\tan\beta$, large δ and lighter charged-Higgs boson, as can be seen from the numerical results in Table I and illustrated explicitly by Figs. 4 and 5. But they tend to cancel each other and finally lead to a small change to the prediction for the branching ratio under study.

It is worth noting that both the real and imaginary parts of effective Wilson coefficients are taken into account in our calculation of the branching ratio.

As shown in Eq. (16), the differential decay rate depends on the summation of three terms:

$$\begin{aligned} &\text{Term} - 1\text{: } (1 + 2\hat{s})(|\tilde{C}_{9V}^{\rm eff}(\hat{s})|^2 + |\tilde{C}_{10A}^{\rm eff}(\hat{s})|^2), \\ &\text{Term} - 2\text{: } 4\left(1 + \frac{2}{\hat{s}}\right)|\tilde{C}_{7\gamma}^{\rm eff}|^2, \\ &\text{Term} - 3\text{: } 12\,\mathrm{Re}[\tilde{C}_{7\gamma}^{\rm eff}(\tilde{C}_{9V}^{\rm eff}(\hat{s}))^*], \end{aligned} \tag{36}$$

where the third term is the interference term, which has opposite sign compared to first two terms. From Fig. 6, one can see easily that

(1) After the inclusion of new physics contributions in T2HDM, the signs of three terms remain unchanged.
(2) The new physics contributions to these three terms are indeed tend to cancel each other and result in a summation (solid curve in Fig. 6) which becomes closer to the SM prediction (solid line in Fig. 6) when m_H becoming larger. The theoretical predictions for the branching ratio in the SM and T2HDM agree well for the whole range of m_H considered here. They are also in good agreement with the data within 1 standard deviation.

Analogous to Fig. 6, the Figs. 7 and 8 show the $\tan\beta$ and $\delta-$ dependence of the branching ratio $\mathrm{Br}(B \to X_s l^+ l^-)$, respectively. Here, the cancelation of new physics contributions to different terms occurs and leaves the summation, the theoretical prediction in the T2HDM, in good agreement with the SM prediction as well as the measured value

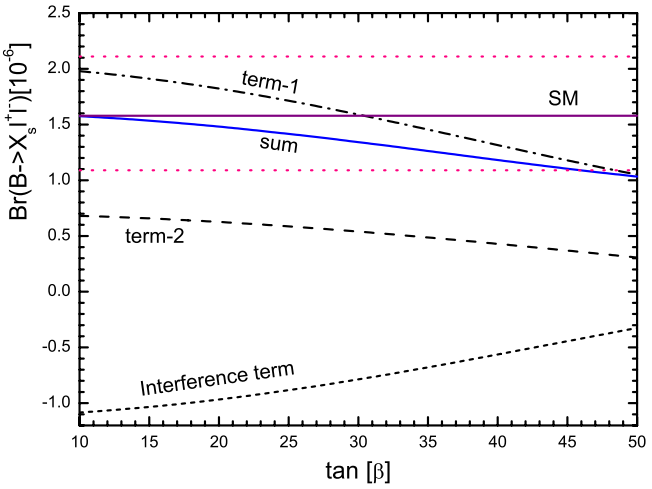

FIG. 7 (color online). The same as Fig. 6, but shows the $\tan\beta$ dependence of the branching ratio of $B \to X_s l^+ l^-$ in the SM and T2HDM for $\delta = 0°$ and $m_H = 300$ GeV.

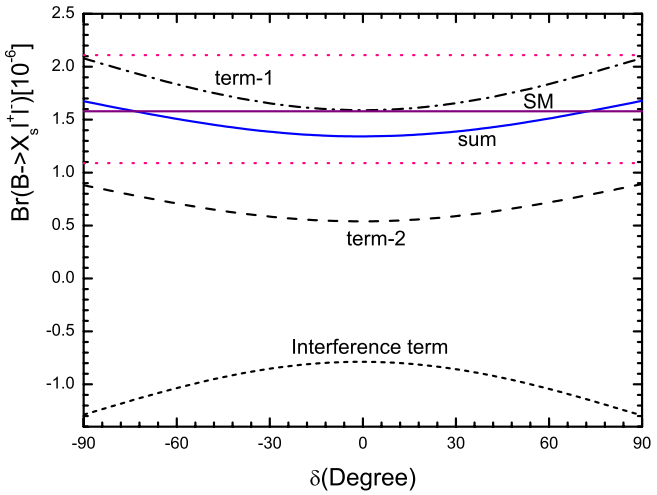

FIG. 8 (color online). The same as Fig. 6, but shows the δ dependence of the branching ratio of $B \to X_s l^+ l^-$ in the SM and T2HDM for $\tan\beta = 30$ and $m_H = 300$ GeV.

within 1 standard deviation. From Fig. 7, one can also see that a $\tan\beta$ smaller than 40 is preferred by current data.

IV. SUMMARY

In this paper, we calculate the new physics contributions to the branching ratio of $B \to X_s\gamma$ and $B \to X_s l^+ l^-$ decays induced by the charged-Higgs loop diagrams in the top-quark two-Higgs-doublet model, and compare the theoretical predictions in the T2HDM with currently available data.

In Sec. II, we firstly present a brief review about the basic structure of the top-quark two-Higgs-doublet model, and then evaluate analytically the new Feynman diagrams induced by the charged-Higgs $H^\pm$ exchanges and extract the new physics parts of the Wilson coefficients $C_{7\gamma}^{\rm NP}(\mu_W)$, $C_{8g}^{\rm NP}(\mu_W)$, $C_{9V}^{\rm NP}(\mu_W)$ and $C_{10A}^{\rm NP}(\mu_W)$ which govern the new physics contributions to $B \to X_s\gamma$ and $B \to X_s l^+ l^-$ decays considered in this paper. For the SM part, we use the known analytical formulae at NNLO level as given, for example, in Refs. [5,17]. The new physics contributions are included through the modifications to the corresponding Wilson coefficients at matching scale $\mu_W \sim M_W$.

From the numerical results and the figures as shown in Sec. III, we found that

(1) For the T2HDM studied here, a light charged-Higgs boson with a mass less than 200 GeV is excluded by the data of $B \to X_s\gamma$ decay at 3σ level. But a charged-Higgs boson with a mass heavier than 300 GeV is still allowed by the data of both $B \to X_s\gamma$ and $B \to X_s l^+ l^-$ decay. The data of $B \to X_s\gamma$ also prefer a small δ, a new CP violating phase appeared in the Yukawa couplings of the T2HDM.

(2) After the inclusion of new physics contributions, the effective Wilson coefficients $\tilde{C}_i^{\rm eff}(m_b)$ $(i = 7\gamma, 9V$ and $10A)$, which govern the branching ratio of $B \to X_s l^+ l^-$ decay, are always SM-like within the considered parameter space of T2HDM. The sign of the interference term in Eq. (16) remains unchanged.

(3) The new physics contributions to $\tilde{C}_{7\gamma}^{\rm eff}$ and $\tilde{C}_{9V}^{\rm eff}$ can be significant in magnitude, respectively, for large $\tan\beta$, large δ and lighter charged-Higgs boson, but they tend to cancel each other and finally result in only a small change to the prediction for the branching ratio of $B \to X_s l^+ l^-$ decay. This feature can be seen clearly through the numerical results in Table I and the curves shown in last three figures.

(4) Within the considered parameter space of the T2HDM, the T2HDM predictions for $\mathrm{Br}(B \to X_s l^+ l^-)$ agree well with the SM as well as the measured value within 1 standard deviation.

ACKNOWLEDGMENTS

This work is partly supported by the National Natural Science Foundation of China under Grant No. 10275035, 10575052, and by the Specialized Research Fund for the Doctoral Program of higher education (SRFDP) under Grant No. 20050319008.

APPENDIX: Br($B \to X_s\gamma$) IN THE SM AND T2HDM

The branching ratio of $B \to X_s\gamma$ at the next-to-leading order (NLO) in the SM and the leading order (LO) in the T2HDM can be written as [19,22]

$$\mathcal{B}(B \to X_s\gamma) = \mathcal{B}_{SL}\left|\frac{V_{ts}^* V_{tb}}{V_{cb}}\right|^2 \frac{6\alpha_{\rm em}}{\pi f(z)\kappa(z)}[|\bar{D}|^2 + A + \triangle], \tag{A1}$$

where $\mathcal{B}_{\rm SL} = 10.61\%$ is the measured semileptonic branching ratio of B meson, $\alpha_{\rm em} = 1/128$ is the fine-structure constant, $z = m_c^{\rm pole}/m_b^{\rm pole} = 0.29 \pm 0.02$ is the ratio of the quark pole mass. The function $f(z)$ and $\kappa(z)$ have been given in Eqs. (25) and (26).

The term $\bar{D}$ at low energy scale $\mu = \mathcal{O}(m_b)$ in Eq. (A1) corresponds to the subprocess $b \to s\gamma$

$$\bar{D} = C_{7\gamma}^{\rm SM}(\mu) + V(\mu) + C_{7\gamma}^{\rm NP}(\mu). \tag{A2}$$

Here $C_{7\gamma}^{\rm SM}(\mu)$ denotes the SM part of the Wilson coefficient $C_{7\gamma}(\mu)$ at NLO level, and the explicit expression of $C_{7\gamma}^{\rm SM}(\mu)$ at both LO and NLO level can be found easily in Ref. [15].

The new physics part of the Wilson coefficient $C_{7\gamma}$ and C_{8g} at the matching scale M_W are currently known at LO level and have been given in Eqs. (7) and (8). At the low energy scale $\mu = \mathcal{O}(m_b)$, the leading order Wilson coefficients $C_{7\gamma}^{\rm NP}(\mu)$ and $C_{8g}^{\rm NP}(\mu)$ can be written as

$$C_{7\gamma}^{\rm NP}(\mu) = \eta^{16/23} C_{7\gamma}^{\rm NP}(M_W) + \frac{8}{3}(\eta^{14/23} - \eta^{16/23}) C_{8g}^{\rm NP}(M_W), \quad \text{(A3)}$$

$$C_{8g}^{\rm NP}(\mu) = \eta^{14/23} C_{8g}^{\rm NP}(M_W), \quad \text{(A4)}$$

where $\eta = \alpha_s(M_W)/\alpha_s(\mu)$, and the Wilson coefficient $C_{8g}^{\rm NP}(M_W)$ has been given in Eq. (8).

The function $V(\mu)$ in Eq. (A1) is defined as [22]

$$V(\mu) = \frac{\alpha_s(\mu)}{4\pi}\left\{\sum_{i=1}^{8} C_i^0(\mu)\left[r_i + \frac{1}{2}\gamma_{i7}^0 \ln\frac{m_b^2}{\mu^2}\right] - \frac{16}{3}C_{7\gamma}^0(\mu)\right\}, \quad \text{(A5)}$$

where the functions r_i $(i = 1, \ldots, 8)$ are the virtual correction functions (see Appendix D of Ref. [22]), γ_{i7}^0 are the elements of the anomalous dimension matrix which govern the evolution of the Wilson coefficients from the matching scale M_W to lower scale μ. The values of γ_{i7}^0 can be found in Ref. [22].

In Eq. (A1), the term $A = A(\mu)$ is the correction coming from the bremsstrahlung process $b \to s\gamma g$ [23]

$$A(\mu) = \frac{\alpha_s(\mu)}{\pi}\sum_{i,j=1;i\le j}^{8} \mathrm{Re}\{C_i^0(\mu)[C_j^0(\mu)]^* f_{ij}\}. \quad \text{(A6)}$$

The coefficients f_{ij} have been defined and computed in Refs. [23,24]. We here use the explicit expressions of those relevant f_{ij} as given in Appendix E of Ref. [22].

Finally, the term Δ in Eq. (A1) denotes the nonperturbative corrections [25,26],

$$\Delta = \frac{\delta_\gamma^{\rm NP}}{m_b^2}|C_7^0(\mu)|^2 + \frac{\delta_c^{\rm NP}}{m_c^2}\mathrm{Re}\left\{[C_7^0(\mu)]^* \cdot \left[C_2^0(\mu) - \frac{1}{6}C_1^0(\mu)\right]\right\}, \quad \text{(A7)}$$

with

$$\delta_\gamma^{\rm NP} = \frac{\lambda_1}{2} - \frac{9}{2}\lambda_2, \qquad \delta_c^{\rm NP} = -\frac{\lambda_2}{9}, \quad \text{(A8)}$$

where $\lambda_2 = (m_{B^*}^2 - m_B^2)/4 = 0.12\ \mathrm{GeV}^2$ and $\lambda_1 = 0.5\ \mathrm{GeV}^2$.

In the expressions of $V(\mu)$, $A(\mu)$ and Δ, the superscript "0" means that the corresponding Wilson coefficients at LO level will be used. The numerical results show that the new physics contributions to "small quantities" $A(\mu)$ and Δ are very small in magnitude and can be neglected safely.

[1] E. Barberio *et al.* (Heavy Flavor Averaging Group), hep-ex/0603003.

[2] K. Chetyrkin, M. Misiak, and M. Münz, Phys. Lett. B **400**, 206 (1997); **425**, 414(E) (1998); P. Gambino and M. Misiak, Nucl. Phys. **B611**, 338 (2001); A. J. Buras, A. Czarnecki, M. Misiak, and J. Urban, Nucl. Phys. **B631**, 219 (2002); A. J. Buras, A. Poschenrieder, M. Spranger, and A. Weiler, Nucl. Phys. **B678**, 455 (2004).

[3] P. Gambino, U. Haisch, and M. Misiak, Phys. Rev. Lett. **94**, 061803 (2005).

[4] M. Misiak, Nucl. Phys. **B393**, 23 (1993); **B439**, 461(E) (1995); B. Grinstein, M. J. Savage, and M. B. Wise, Nucl. Phys. **B319**, 271 (1989); R. Grigjanis, P. J. O'Donnell, M. Sutherland, and H. Navelet, Phys. Lett. B **223**, 239 (1989).

[5] A. J. Buras, M. Münz, Phys. Rev. D **52**, 186 (1995).

[6] Y. B. Dai, C. S. Huang, and H. W. Huang, Phys. Lett. B **390**, 257 (1997); S. Schilling, C. Greub, N. Salzmann, and B. Tödtli, Phys. Lett. B **616**, 93 (2005).

[7] A. Ali, E. Lunghi, C. Greub, and G. Hiller, Phys. Rev. D **66**, 034002 (2002).

[8] C. Bobeth, A. J. Buras, F. Früger, and J. Urban, Nucl. Phys. **B630**, 87 (2002); C. Bobeth, A. J. Buras, and T. Ewerth, Nucl. Phys. **B713**, 522 (2005).

[9] A. Das and C. Kao, Phys. Lett. B **372**, 106 (1996).

[10] K. Kiers, A. Soni, and G. H. Wu, Phys. Rev. D **59**, 096001 (1999); G. H. Wu and A. Soni, Phys. Rev. D **62**, 056005 (2000).

[11] K. Kiers, A. Soni, and G-H. Wu, Phys. Rev. D **62**, 116004 (2000).

[12] W.-S. Hou, Phys. Lett. B **296**, 179 (1992); M. Luke and M. J. Savage, Phys. Lett. B **307**, 387 (1993); D. Atwood, L. Reina, and A. Soni, Phys. Rev. D **55**, 3156 (1997); M. Sher, *Proceedings of the 29th International Conference on High-Energy Physics (ICHEP98)* (Vancouver, Canada, 1998).

[13] M. Kobayashi and T. Maskawa, Prog. Theor. Phys. **49**, 652 (1973).

[14] A. J. Buras, in *Probing the Standard Model of Particle Interactions*, edited by F. David and R. Gupta (Elsevier Science B.V., New York, 1998); hep-ph/9806471.

[15] G. Buchalla, A. J. Buras, and M. E. Lautenbacher, Rev. Mod. Phys. **68**, 1125 (1996).

[16] T. Inami and C. S. Lim, Prog. Theor. Phys. **65**, 297 (1981); **65**, 1772(E) (1981).

[17] C. Bobeth, M. Misiak, and J. Urban, Nucl. Phys. **B574**, 291 (2000); C. Bobeth, P. Gambino, M. Gorbahn, and U. Haisch, J. High Energy Phys. 04 (2004) 071.

[18] S. Eidelman *et al.* (Particle Data Group), Phys. Lett. B **592**, 1 (2004).

[19] Z. J. Xiao, H. H. Cheng, and L. X. Lü, hep-ph/0512359.

[20] B. Aubert *et al.* (*BABAR* Collaboration), Phys. Rev. Lett. **93**, 081802 (2004).

[21] M. Iwasaki *et al.* (Belle Collaboration), Phys. Rev. D **72**, 092005 (2005); K. Abe *et al.* (Belle Collaboration), hep-ex/0508009.

[22] F. M. Borzumati and C. Greub, Phys. Rev. D **58**, 074004 (1998); **59**, 057501 (1999).

[23] A. Ali and C. Greub, Z. Phys. C **49**, 431 (1991); Phys. Lett. B **259**, 182 (1991); **361**, 146 (1995); N. Pott, Phys. Rev. D **54**, 938 (1996).

[24] K. G. Chetyrkin, M. Misiak, and M. Munz, Phys. Lett. B **400**, 206 (1997); **425**, 414(E) (1998).

[25] A. Falk, M. Luke, and M. Savage, Phys. Rev. D **49**, 3367 (1994).

[26] M. B. Voloshin, Phys. Lett. B **397**, 275 (1997); Z. Ligeti, L. Randall, and M. B. Wise, Phys. Lett. B **402**, 178 (1997); A. K. Grant, A. G. Morgan, S. Nussinov, and R. D. Peccei, Phys. Rev. D **56**, 3151 (1997); G. Buchalla, G. Isidori, and S. J. Rey, Nucl. Phys. **B511**, 594 (1998).